

# Multiplexed RNAscope and immunofluorescence on whole-mount skeletal myofibers and their associated stem cells

Allison P. Kann<sup>1,2</sup> and Robert S. Krauss<sup>1,2,\*</sup>

## ABSTRACT

Skeletal muscle myofibers are large syncytial cells comprising hundreds of myonuclei, and *in situ* hybridization experiments have reported a range of transcript localization patterns within them. Although some transcripts are uniformly distributed throughout myofibers, proximity to specialized regions can affect the programming of myonuclei and functional compartmentalization of transcripts. Established techniques are limited by a lack of both sensitivity and spatial resolution, restricting the ability to identify different patterns of gene expression. In this study, we adapted RNAscope fluorescent *in situ* hybridization technology for use on whole-mount mouse primary myofibers, a preparation that isolates single myofibers with their associated muscle stem cells remaining in their niche. This method can be combined with immunofluorescence, enabling an unparalleled ability to visualize and quantify transcripts and proteins across the length and depth of skeletal myofibers and their associated stem cells. Using this approach, we demonstrate a range of potential uses, including the visualization of specialized transcriptional programming within myofibers, tracking activation-induced transcriptional changes, quantification of stem cell heterogeneity and evaluation of stem cell niche factor transcription patterns.

**KEY WORDS:** Imaging, Muscle stem cell, Skeletal muscle, Satellite cells, Fluorescent *in situ* hybridization, Mouse

## INTRODUCTION

Skeletal myofibers are large multinucleated cells formed through the fusion of mononuclear myoblasts. Upon fusion, the cells experience an extensive reorganization of cellular components to allow the formation of contractile myofibrils, including the repositioning of nuclei to the periphery of the cell (Bruusgaard et al., 2006), modification of the endoplasmic reticulum to form the net-like sarcoplasmic reticulum, redistribution of microtubule organizing centers (Tassin et al., 1985) and the restructuring of endoplasmic reticulum (ER)-to-Golgi trafficking (Nevalainen et al., 2010). Although the unique cellular structure of myofibers prompts interesting questions of how basic transcriptional and translational functions are regulated, addressing these requires innovation and adaptation of classical techniques.

Transcript distribution within adult skeletal muscle has been reported using traditional *in situ* hybridization methods on sectioned


muscle, showing a range of mRNA localization patterns for dystrophin, various myosin heavy chains, calsequestrin and dihydropyridine receptors (Mitsui et al., 1997; Shoemaker et al., 1999; Nissinen et al., 2005). Whereas most such studies have analyzed uniformly expressed muscle genes and their locations within the depth of myofibers, there is also evidence that gene expression patterns of myonuclei can vary depending on their position along myofibers and proximity to specialized regions. This specialization and functional compartmentalization of transcripts has been most extensively studied at the neuromuscular junction (NMJ), where NMJ-specific genes are locally transcribed by synaptic myonuclei (Merlie and Sanes, 1985; Fontaine et al., 1988; Jasmin et al., 1993; Jevsek et al., 2006; Moscoso et al., 1995; Sanes et al., 1991). These transcripts do not diffuse throughout the sarcoplasm; instead, they are preferentially translated near their nucleus of origin for local assembly and utilization (Rossi and Rotundo, 1992). Although the exact mechanisms by which this localization occurs remain unknown, locally derived post-transcriptional signals from the NMJ are likely involved (reviewed by Chakkalakal and Jasmin, 2002).

Besides motor neurons at the NMJ, the only other cells known to form stable contacts with adult myofibers are satellite cells (although it is possible that some interstitial cells may also do so). Satellite cells (SCs) are adult skeletal muscle stem cells and the driving force behind regenerative myogenesis. They are small mononuclear polarized cells that reside between apical myofibers and the surrounding basal lamina (Brack and Rando, 2012; Dumont et al., 2015). Upon injury, SCs activate, proliferate and fuse into the myofiber to repair muscle damage. Although there is no known specialization of the myofiber area in contact with SCs as seen in the subsynaptic region of the NMJ, the myofiber is a niche cell for SCs, indicating that they communicate with each other (Goel et al., 2017; Sampath et al., 2018; Mashinchian et al., 2018).

We sought to develop a technique to examine whether the myonuclei that reside adjacent to SCs are transcriptionally programmed in a manner similar to synaptic myonuclei. Although RNA sequencing of isolated SCs has become a standard protocol (Pallafacchina et al., 2010; Machado et al., 2017; van Velthoven et al., 2017), we needed a method by which we could observe the transcriptional activity of the specific myonuclei near SCs. This spatial factor can be addressed using single primary myofiber preparations, an essential technique in the SC field typically used for whole-mount immunofluorescence (IF). Introduced thirty years ago (Bischoff, 1986) and adapted by numerous groups since (Rosenblatt et al., 1995; Zammit et al., 2004; Keire et al., 2013), this protocol teases mouse extensor digitorum longus (EDL) muscles into individual myofibers, complete with SCs remaining in their physical niche. Previous mRNA localization studies have used a variety of techniques, ranging from traditional DIG-labeled probes or radioactive labeling to more recent small-molecule fluorescent *in situ* hybridization (smFISH) studies on SCs (Crist et al., 2012;

<sup>1</sup>Department of Cell, Developmental, and Regenerative Biology, Icahn School of Medicine at Mount Sinai, New York, NY 10029, USA. <sup>2</sup>Graduate School of Biomedical Sciences, Icahn School of Medicine at Mount Sinai, New York, NY 10029, USA.

\*Author for correspondence (Robert.Krauss@mssm.edu)

 A.P.K., 0000-0003-0111-9081; R.S.K., 0000-0002-7661-3335

Chakkalakal et al., 2012; de Morrée et al., 2017; Gayraud-Morel et al., 2018). However, the field still lacks a rigorous, sensitive method by which single transcripts can be identified and quantified across whole myofibers and SCs.

To investigate mechanisms of transcriptional regulation within the myofiber and to quantify SC transcriptional heterogeneity, we adapted RNAscope fluorescent *in situ* hybridization technology (Wang et al., 2012) for use on both freshly isolated and cultured primary myofibers. Here, we report a whole-mount myofiber-RNAscope (MF-RNAscope) protocol that can be multiplexed with IF for the simultaneous visualization and quantification of single transcripts and proteins throughout primary skeletal myofibers and their associated SCs.

## RESULTS AND DISCUSSION

### MF-RNAscope allows sensitive detection of RNAs within skeletal myofibers

ACDBio's RNAscope technique allows for sensitive detection of multiple transcripts at high resolution (Wang et al., 2012) and has been adapted for a variety of cell types and preparations since its development. Most notably, the RNAscope fluorescent protocol has been adapted for whole-mount use on zebrafish embryos (Gross-Thebing et al., 2014), as well as thick tissue sections (Kersigo et al., 2018). However, when trying to establish a protocol for whole-mount myofiber preparations, all of the published protocols yielded high levels of non-specific signals (Fig. S1A). We therefore developed a protocol using the RNAscope Multiplex Fluorescent v2 system that reduced background noise and allowed analysis of both the full depth of myofibers and their associated SCs, thus expanding the technology to allow an unprecedented spatial and quantifiable analysis of transcription patterns across primary myofibers (Fig. S1B-D, see Materials and Methods).

Once we established a working protocol on myofibers, we tested the specificity of the technique by probing for acetylcholinesterase

(*Ache*), a gene known to be locally transcribed by and sequestered near synaptic myonuclei at the NMJ (Rotundo, 1990; Rossi and Rotundo, 1992). As expected, MF-RNAscope showed *Ache* RNA tightly clustered in and around the NMJ (Fig. 1A), easily identified by the distinctive cluster of synaptic nuclei within myofibers (Fig. S2A,B). This regional localization was in sharp contrast to the expression of myosin heavy chain (*Myh2*) RNA, which was seen in high concentrations throughout the entire length and depth of myofibers (Fig. 1A; Movie 1).

Isolation of myofibers and subsequent culturing with chick embryo extract (CEE) is a standard technique in the field, extensively used to study SC activation (Zammit et al., 2004; Vogler et al., 2016; Goel and Krauss, 2018). Here, we show that MF-RNAscope reveals activation-induced transcriptional changes throughout myofibers. *Myod1*, encoding the key muscle-specific transcription factor MyoD, is transcribed by SCs during quiescence but only translated upon activation (Crist et al., 2012; Hausburg et al., 2015; de Morrée et al., 2017). Although known to be crucial in SC biology, the role and distribution of *Myod1* transcripts within cultured myofibers has not, as far as we are aware, been studied. Within freshly isolated myofibers (0 h/T0), *Myod1* transcripts were localized in and around myonuclei (Fig. 1B). Upon culture with CEE for 24 h (T24), *Myod1* transcripts within myofibers increased twofold (Fig. 1C,D). We observed a similar, larger increase in *Myod1* transcript levels within SCs at T24 (Fig. S3A,B). Interestingly, at T24 MyoD protein is only produced by SCs and is not detectable within myofibers (Collins et al., 2007; Goel et al., 2017), suggesting a post-transcriptional mechanism of *Myod1* regulation within myofibers.

### MF-RNAscope can be used to quantify SC transcriptional heterogeneity without SC isolation

Although initially proposed as a homogenous group of cells, it is now recognized that SCs comprise a heterogenous population

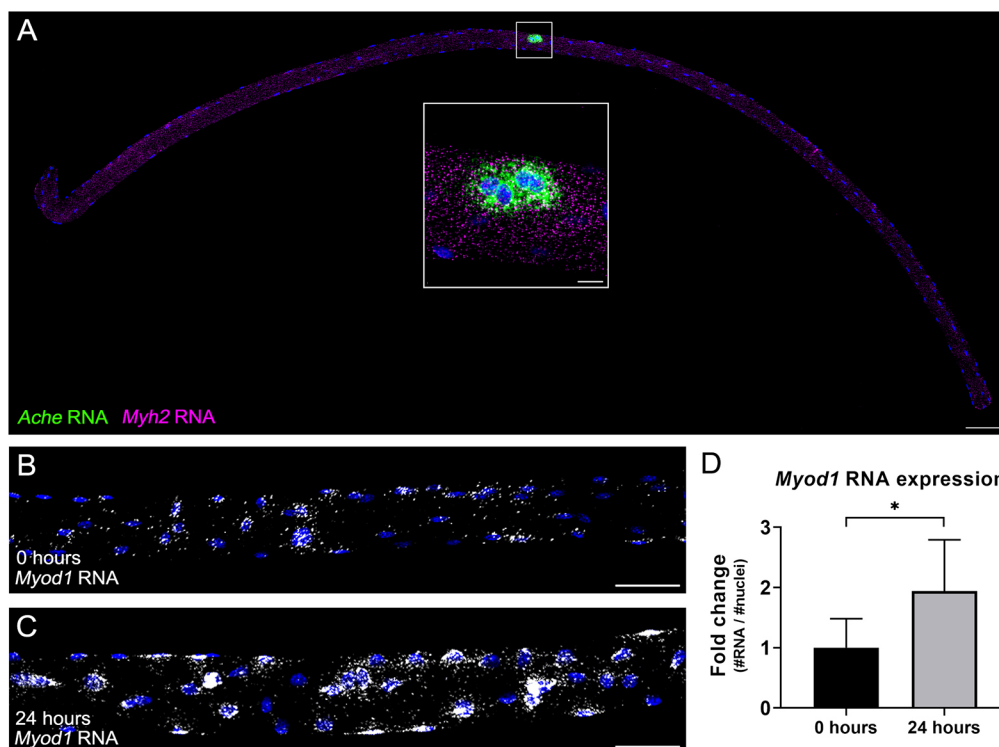


**Fig. 1. MF-RNAscope allows sensitive detection of RNAs within myofibers.** (A) MF-RNAscope of a myofiber probed for *Ache* (green) and *Myh2* (magenta) RNAs. Image is a tile-stitched maximum intensity projection of confocal images throughout the myofiber (20× magnification). (B,C) MF-RNAscope for *Myod1* RNA on a freshly isolated fiber (B) and a fiber cultured for 24 h in CEE medium (C). Images are maximum intensity projections. (D) Fold change quantification of *Myod1* RNA across myofibers at T0 and T24. Ratios of the number of RNA molecules in the fiber/number of nuclei in the fiber were calculated for both time points, then standardized to the T0 value. Error bars represent s.d.; \* $P < 0.0001$  (Welch's unpaired two-tailed *t*-test). For additional details, see Materials and Methods. Nuclei are identified with DAPI (blue). Scale bars: 100  $\mu$ m in A; 10  $\mu$ m in A, inset; 50  $\mu$ m in B,C.

(Olguin and Olwin, 2004; Zammit et al., 2004; Shinin et al., 2006; Kuang et al., 2007; Tanaka et al., 2009; Rocheteau et al., 2012; Dell'Orso et al., 2019). SmFISH experiments have been performed on SCs (Crist et al., 2012; de Morrée et al., 2017; Gayraud-Morel et al., 2018), but generally require isolation and removal of the SCs from their niche to achieve quantifiable results. Given the established role of niche components in SC regulation (reviewed by Mashinchian et al., 2018), a means to study transcriptional changes while minimizing niche disruption is crucial. MF-RNAscope maintains SCs underneath the basal lamina, allowing for the study of SC transcriptional heterogeneity without physical removal from their niche. We used MF-RNAscope to probe expression of a panel of

known SC markers and niche components, quantifying numbers of transcripts per SC for *Pax7*, *Myod1*, *Myf5*, *Cd34*, *Vcam1*, *Sdc4*, *Cdh15*, *Cdh2* and *Cdh5* (Fig. 2A). Although we cannot ensure that the puncta represent every transcript, our results (Fig. 2B) demonstrate a range of transcript numbers per quiescent SC similar to those previously reported for specific genes in isolated cells (de Morrée et al., 2017) and percentages of positive SCs seen with isolated fibers (Beauchamp et al., 2000).

Although expression of *Pax7* or *Sdc4* RNA was sufficient to label quiescent SCs, we adapted MF-RNAscope to incorporate the multiplexing with IF (see Materials and Methods), allowing increased flexibility in experimental design. MF-RNAscope/IF

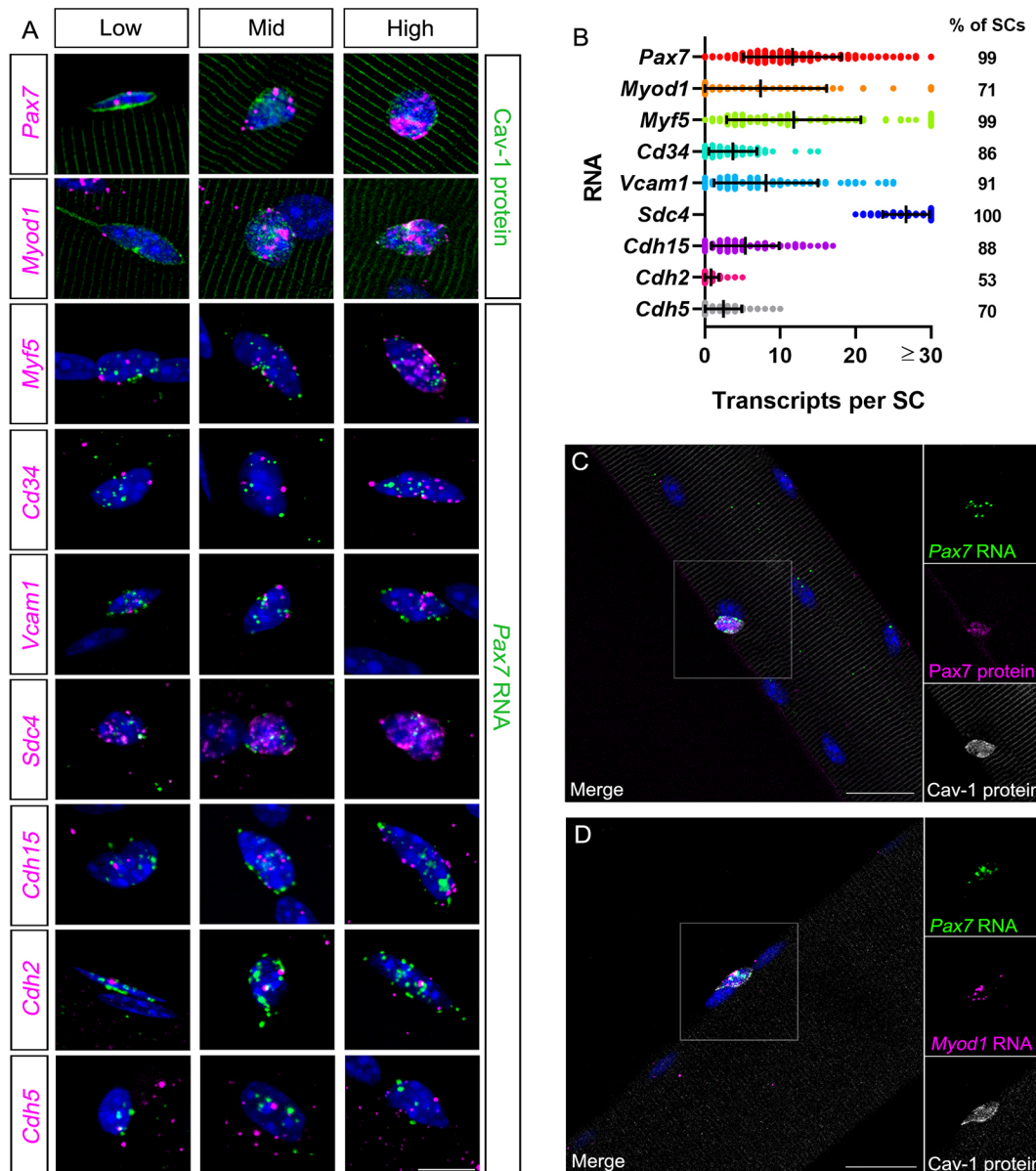


**Fig. 2. MF-RNAscope can be used alone or in combination with IF to evaluate and quantify SC heterogeneity.** (A) MF-RNAscope or MF-RNAscope/IF of SCs on myofibers probed for (top to bottom, in magenta): *Pax7*, *Myod1*, *Myf5*, *Cd34*, *Vcam1*, *Sdc4*, *Cdh15*, *Cdh2* and *Cdh5* RNAs. All SCs were identified through a multiplexed SC marker (green), either Cav1 protein (top two rows) or Pax7 RNA (remaining rows). Each row contains SCs with low, mid and high levels of the given RNAs. (B) Quantification of transcripts per SC; right column indicates the percentage of SCs with  $\geq 1$  visible transcript. The numbers of individual puncta are listed as transcripts. Data are mean $\pm$ s.d.  $n=225$  (*Pax7*), 73 (*Myod1*), 93 (*Myf5*), 83 (*Cd34*), 80 (*Vcam1*), 76 (*Sdc4*), 91 (*Cdh15*), 91 (*Cdh2*) and 84 (*Cdh5*) SCs from  $\geq 3$  mice each. (C,D) MF-RNAscope/IF of SCs: *Pax7* RNA (green), Pax7 (magenta) and Cav1 (white) proteins (C); Pax7 (green) and MyoD (magenta) RNAs and Cav1 protein (white) (D). Note that the Cav1 antibody interacts non-specifically and variably with sarcomeres. Nuclei are identified with DAPI (blue). Insets (right) show magnification of boxed area. Scale bars: 10  $\mu$ m in A; 25  $\mu$ m in C,D.



can be used in multiple combinations; here, we show *Pax7* RNA with Pax7 and caveolin 1 (Cav1) protein (Fig. 2C), as well as *Pax7* and *Myod1* RNAs with Cav1 protein (Fig. 2D). MF-RNAscope thus introduces a method by which to analyze the heterogeneity of transcript levels within SCs – one that includes spatial information and maintains SCs in their niche.

### Transcriptional patterns of myofiber-derived niche components can be evaluated and quantified using MF-RNAscope

Using MF-RNAscope, we detected several patterns of transcript localization within myofibers. *Myh2* transcripts were uniformly distributed throughout the fiber sarcoplasm, *Ache* transcripts were tightly clustered at the NMJ and *Myod1* transcripts were clustered in and around most myonuclei. We therefore used this technique to test potential interactions between myofibers and SCs. The myofiber acts as a niche cell for the SC and provides several factors that regulate SC quiescence, including classical cadherins that facilitate the SC-myofiber adherent junction (Goel et al., 2017). The consistent presence of

myonuclei near SCs has been reported (Christov et al., 2007), but whether these so-called ‘paired’ myonuclei are programmed to specifically communicate with SCs has never been tested. Classical cadherins are involved in differentiation and fusion of myoblasts during muscle development (Krauss et al., 2017), but by the adult stage they become restricted to the SC-myofiber junction (Irintchev et al., 1994; Goel et al., 2017).

Given this strict localization of cadherin proteins to the adult niche (Fig. 3A; Goel et al., 2017), we hypothesized that cadherin RNAs might be locally transcribed in and sequestered near paired myonuclei in a manner analogous to NMJ components and synaptic nuclei. There are at least three cadherins detectable at the SC niche: M-cadherin (encoded by *Cdh15*), N-cadherin (*Cdh2*) and VE-cadherin (*Cdh5*). In contrast to the tightly localized expression of the cadherin proteins, all three *Cdh* transcripts were evenly distributed throughout the entire myofiber (Fig. 3C,D; Fig. S4A). To confirm that this expression pattern was specific, we performed the same experiment on myofibers from mice lacking N- and M-cadherin [*Mcad*<sup>-/-</sup>; *Ncad*<sup>fl/fl</sup>; *MyoD*<sup>Cre</sup>] (Goel et al., 2017), IF

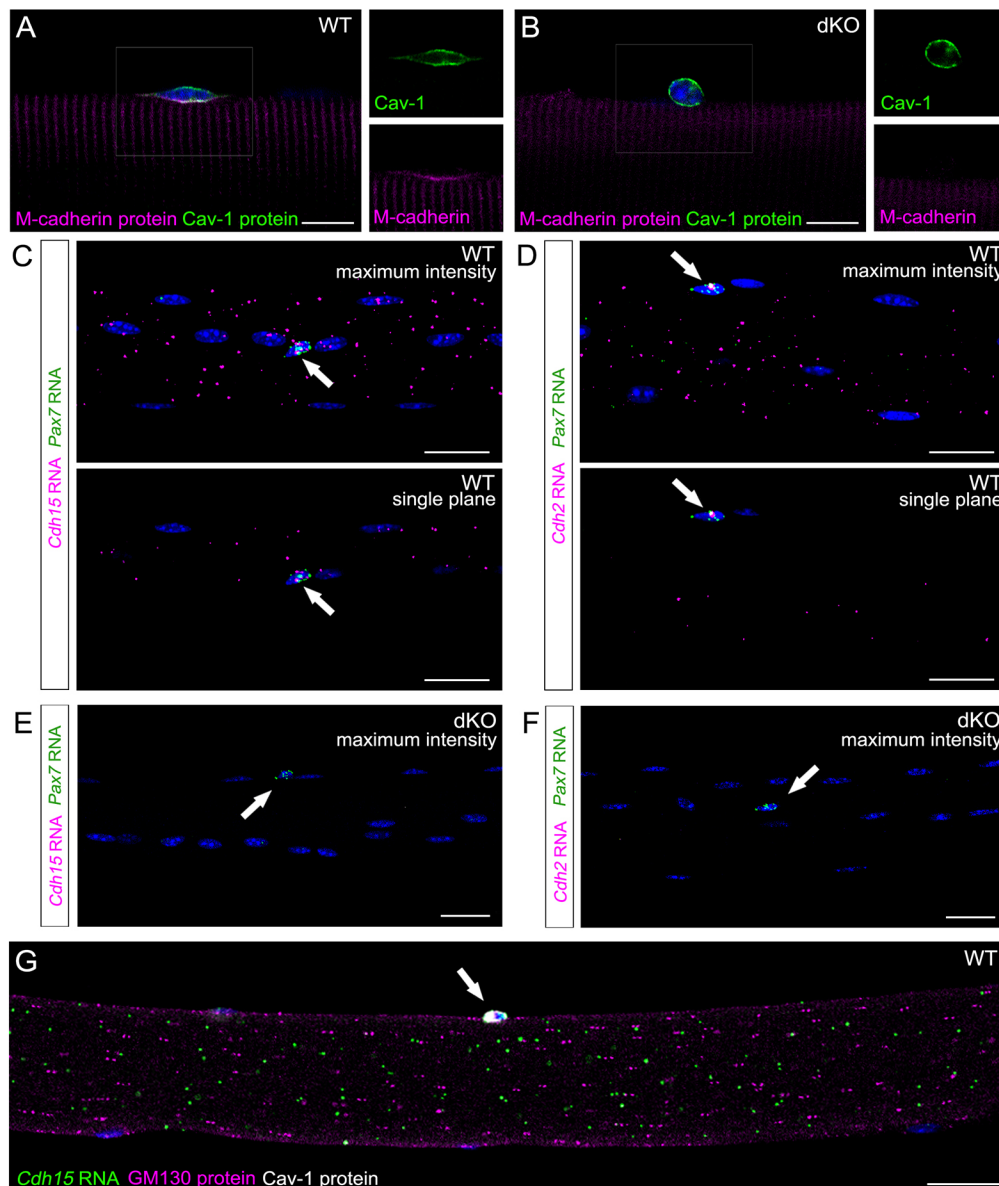


**Fig. 3. Niche cadherin transcripts are distributed evenly throughout the length and depth of myofibers.**

(A,B) IF of myofibers from wild-type (WT; A) or *MyoD*<sup>Cre</sup>; *Cdh2*<sup>fl/fl</sup>; *Cdh15*<sup>-/-</sup> (dKO; B) mice stained for M-cadherin (magenta) and Cav1 (green). Note that M-cadherin signal at the apical membrane of the SC is specifically lost in dKO fibers. Insets (right) show magnification of boxed area. (C,D) MF-RNAscope of myofibers probed for *Pax7* (green) and *Cdh15* (C) or *Cdh2* (D) RNAs (magenta). Top images show maximum intensity projections (40× magnification). Bottom images show single confocal planes. Arrows indicate *Pax7*<sup>+</sup> SCs. (E,F) MF-RNAscope of dKO myofibers probed for *Pax7* (green) and *Cdh15* (E) or *Cdh2* (F) RNAs (magenta). Images are maximum intensity projections. Arrows indicate *Pax7*<sup>+</sup> SCs. (G) MF-RNAscope/IF of myofibers probed for *Cdh15* RNA (green) and stained for GM130 (magenta) and Cav1 (white) proteins. Image is a single confocal plane in the middle of the myofiber. Arrow indicates a Cav1<sup>+</sup> SC. Nuclei are identified with DAPI (blue). Scale bars: 10 μm in A,B; 25 μm in C-G.

shown in Fig. 3B], and saw the expected loss of signal (Fig. 3E,F). We also probed for expression of *Hgf* and *Fgf2*, which encode niche factors that play a role in SC activation (reviewed by Kuang et al., 2008), and observed similar expression patterns to cadherins (Fig. S5A,B). In addition to labeling proteins and RNAs found in SCs, which are present on the exterior of the fiber, we also ensured that the multiplex protocol could identify proteins and RNAs present through the full depth of myofibers. Fig. 3G demonstrates MF-RNAscope for *Cdh15* RNA with IF for GM130 (also known as Golga2; a *cis*-Golgi marker found throughout the myofiber) and Cav1.

To further delve into expression of putative fiber-derived niche factors, we studied a potentially more dynamic protein – the Notch ligand Dll4. Dll4 differs from the cadherins in protein localization; similar to the cadherins, Dll4 was enriched at the SC niche, but in contrast to the cadherins, Dll4 was also observed throughout the fiber in discrete puncta (Fig. 4A): 97% of Dll4 puncta co-stained with the *cis*-Golgi marker GM130 (Fig. 4B, quantification described in Materials and Methods), suggesting they are actively trafficked through the Golgi apparatus.

We next compared transcript localization of these niche factors. As with cadherin transcripts, *Dll4* RNA was seen throughout the length of myofibers (Fig. 4C). Although both cadherin- and Dll4-encoding transcripts were present in nuclei, a higher percentage of *Dll4* transcripts were found in and around myonuclei compared with the cadherins, which were most frequently seen in the cytoplasm

(Fig. 4D). Furthermore, a much higher percentage of myonuclei contained *Dll4* transcripts than any of the cadherin transcripts (Fig. 4E), and the number of transcripts per positive nucleus was higher for *Dll4* than *Cdh2*, *Cdh5* or *Cdh15* (Fig. 4F). These numbers occur despite a lack of substantial variation among total transcript counts (average number of transcripts per 40× image: *Cdh2*=242, *Cdh5*=460, *Cdh15*=343 and *Dll4*=370).

Although cadherins and Dll4 are transmembrane proteins that are established and putative niche factors, respectively, we hypothesize that these differences in nuclear localization and quantity of the respective RNAs are due to the dynamics of the proteins they encode. Cadherins are components of relatively stable junctions, perhaps needing less active transcription for junction maintenance in quiescent SCs. In contrast, abundant Dll4 protein turnover may be required to maintain the high level of Notch signaling required for SC quiescence (Fukada et al., 2011; Bjornson et al., 2012; Mourikis et al., 2012), therefore requiring a higher rate of transcription. This hypothesis would also explain the difference in IF staining: Dll4 was seen in Golgi-derived vesicles throughout myofibers (Fig. 4B), but such puncta were not obviously visible for cadherins. Therefore, the mechanism by which cadherin proteins are specifically localized at the SC niche remains unknown. Although this study revealed that transcript regionalization and specific programming of SC-proximal myonuclei do not occur for the factors analyzed here, it is possible that such a mechanism is operative for other factors. Our

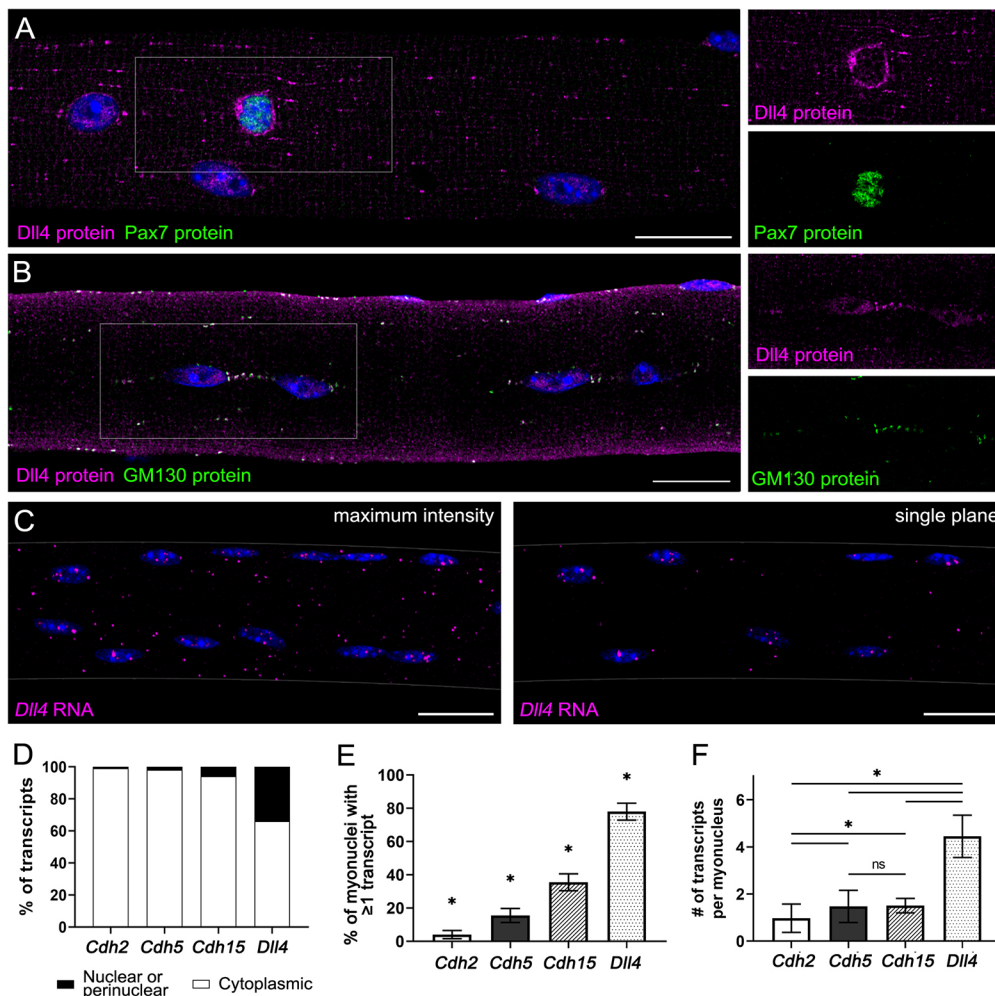


**Fig. 4. Transcriptional patterns of myofiber-derived niche components can be evaluated and quantified using MF-RNAscope.** (A,B) IF of myofibers stained for Dll4 (magenta) and Pax7 (A) or GM130 (B) (green). Insets (right) show magnification of boxed area. (C) MF-RNAscope of a myofiber probed for *Dll4* RNA (magenta), showing a maximum intensity projection (40× magnification; left) and a single confocal plane (right). (D) Quantification of *Cdh2*, *Cdh5*, *Cdh15* and *Dll4* transcript localization. (E) Percentage of myonuclei that contain ≥1 *Cdh2*, *Cdh5*, *Cdh15* or *Dll4* RNA. (F) Average numbers of *Cdh2*, *Cdh5*, *Cdh15* or *Dll4* transcripts per myonucleus. Data are mean±s.d. \* $P < 0.0001$  (two-tailed *t*-tests). compared with all other columns (E) and as indicated (F). ns, not significant. Quantifications represent  $n=3$  mice, 10 fibers/mouse, three 40× z-stacks/fiber. Nuclei are identified with DAPI (blue). Scale bars: 20 μm in A,B; 25 μm in C.

development of MF-RNAscope will allow detection of such specificity. Finally, we point out that, although the probes used in this study were to exonic sequences, it is possible to develop probes to intronic sequences or exon-intron boundaries, enabling the use of MF-RNAscope to study additional phenomena relevant to transcriptional regulation.

## Conclusions

We have shown here that MF-RNAscope is a versatile technique with a wide range of potential uses, including: (1) visualizing and identifying areas of specialized transcriptional activity within entire myofibers; (2) tracking transcriptional changes across whole myofibers in response to extracellular signals; (3) examining and quantifying the heterogeneity of transcripts within SC populations; and (4) comparing production of SC niche factors by evaluating spatial patterns of their transcripts and proteins. By combining the detection capabilities of MF-RNAscope with whole-mount IF on primary myofibers, this protocol allows an unprecedented look into the biology of skeletal muscle.

## MATERIALS AND METHODS

### Mice

This study was carried out in strict accordance with the recommendations in the Guide for the Care and Use of Laboratory Animals of the National Institutes of Health. The protocol was approved by the Icahn School of Medicine at Mount Sinai Institutional Animal Care and Use Committee (IACUC). The Mount Sinai animal facility is accredited by the Association for Assessment and Accreditation of Laboratory Animal Care International (AAALAC). Wild-type C57BL6/J mice were obtained from Jackson Laboratories and *MyoD<sup>Cre</sup>; Cdh2<sup>fl/fl</sup>; Cdh15<sup>-/-</sup>* (dKO) mice were generated as previously described (Goel et al., 2017). All mice were harvested between 2 and 6 months of age; experiments used both male and female mice.

### Single myofiber isolation and culture

Single myofibers were isolated from EDL muscles of adult mice as previously described (Goel and Krauss, 2018). Briefly, EDL muscles were dissected and digested in Type 1 collagenase (Worthington; 2.4 mg/ml) for 1 h in a 37°C shaking water bath. After digestion, muscles were gently triturated for 5 min using a horse serum (HS)-coated wide-mouth Pasteur pipette to dissociate individual myofibers from bulk muscle. Fibers were either immediately collected or cultured in the presence of 0.5% CEE (Thermo Fisher Scientific) for 24 h at 37°C.

### Immunofluorescence

Myofiber IF was performed as described elsewhere (Goel and Krauss, 2018). Briefly, isolated fibers were fixed for 10 min in 4% paraformaldehyde (PFA), washed with PBS, permeabilized for 10 min using PBS plus 0.2% Triton X-100 (PBTX), then blocked for 1 h in 10% goat serum (GS). Primary antibodies were added and fibers were incubated at 4°C overnight. Fibers were washed with PBS and PBTX the following day, blocked for 1 h in 10% GS, then secondary antibodies were added and fibers were incubated for 1 h at room temperature. For reagent and antibody information, see Table S1.

### MF-RNAscope

Before beginning the RNAscope protocol, we recommend becoming familiar with the RNAscope Multiplex Fluorescent Assay v2 (ACDBio, materials available on acdbio.com). Briefly, the assay allows simultaneous visualization of up to three RNA targets, with each probe assigned a different channel (C1, C2 or C3) at the time of purchase. Each channel requires its own amplification steps – for example, a C1 probe will be amplified by horseradish peroxidase (HRP)-C1, followed by the addition of whichever fluorophore will be assigned to that probe/channel, and C1 will then be blocked using an HRP blocker before amplification of the next channel.

### Fixation and dehydration (day 1)

#### Protocol

1. After trituration of myofibers, allow fibers to incubate at 37°C for no more than 10 min to limit any isolation-induced transcriptional activity. Transfer fibers to HS-coated 5 ml tubes and wash 3× with PBS for 5 min. [Note: Only the healthiest fibers can withstand the numerous washes required for the MF-RNAscope protocol. Therefore, when selecting fibers from plates, it is crucial to avoid any bent, wavy or otherwise damaged fibers and select only intact ones.]
2. Fix fibers in 4% paraformaldehyde in PBS in the dark for 10 min, then wash 3× with PBS. [Note: Fibers can be stored in PBS at 4°C for up to 2 weeks.]
3. After fixation, dehydrate myofibers by transferring them from PBS directly to 100% MeOH using a 40 µm cell strainer filter. Agitate gently to ensure that the fibers do not clump together, and allow the fibers to sit in 100% MeOH. Although we have achieved success with leaving fibers in MeOH for only 15 min, we recommend storing them in MeOH at −20°C for at least 2 h for best results. [Note: Fibers can be stored in 100% MeOH at −20°C for up to 6 months.]

### Rehydration and pretreatment (day 1)

#### Protocol

1. Rehydrate fibers in a decreasing methanol/PBS+0.1% Tween-20 (PBST; filter before use) series (50% MeOH/50% PBST; 30% MeOH/70% PBST; 100% PBST) for 5 min each. [Note: For easy transfer and to minimize disturbance of the fibers, use a 40 µm nylon filter and transfer between wells of a six-well untreated tissue culture plate (Fig. S6A). Agitate gently at each step to prevent clumping of fibers.]
2. Once rehydrated, transfer fibers to an Eppendorf tube, 25–30 fibers/tube (we recommend Axygen 1.7 ml tubes for the clarity of the plastic; see Fig. S6B). [Note: When selecting fibers to transfer to Eppendorf tubes, it is again crucial to select only the healthiest fibers. For examples, see Fig. S6C.]
3. Allow fibers to settle to the bottom of each tube, and carefully remove PBST using a transfer pipette. [Note: To ensure maximum control over solution removal and avoid accidental fiber loss, we add a 10 µl pipette tip to the end of each transfer pipette (Fig. S6D) and remove solution while holding each tube up to a light source. Using this apparatus, we can remove almost all of each solution and minimize the dilution of reagents at subsequent steps.]
4. Slowly add 150 µl of Protease 3 (ACD) to the tube and tap gently to mix. Incubate at room temperature on a nutator for 15 min. If multiplexing with IF, this digestion time may need to be shortened (depending on the antibody), but we recommend digesting for no less than 10 min to ensure full penetration of the fibers. We note that protease treatment may destroy certain epitopes, and some antibodies will not work in conjunction with RNAscope. [Note: Agitation steps should be performed on a nutator if possible, as we found that a rocker did not wash the fibers sufficiently. If using a rocker, longer wash times may be required. In this paper, all protein antibodies were used on fibers that were digested for 15 min, except Pax7, which required a shorter digestion time of 10 min. While the fibers are digesting, warm RNAscope probes to 40°C for 10 min, then cool to room temperature before use.]
5. Wash the fibers 3× with 1 ml PBST at room temperature. Each wash should be composed of 3 min on the nutator and 3 min standing upright to allow fibers to settle to the bottom of each tube before removing liquid.
6. Remove as much PBST as possible (leaving no more than 25–50 µl in the tube) and add 125 µl of mixed target probes to each tube. Hybridize overnight (at least 10–12 h) in 40°C water bath. [Note: As detailed in the RNAscope manual, target probes of C1, C2 and/or C3 should be mixed at a 50:1:1 ratio.]



**Amplification (day 2)****Protocol**

1. Remove the tubes from the water bath and wash fibers 3× on a nutator for 10 min with 1 ml 0.2× saline-sodium citrate buffer plus 0.01% Tween-20 (SSCT; filter before use). [Note: For day 2, each wash between steps takes 10 min: 7 min on the nutator followed by 3 min standing upright to allow fibers to settle. Between washes, up to 100 µl of solution may be left in the tube, but before each reagent is added there must be no more than 50 µl in the tube. All amplification/blocking incubation steps occur in a 40°C water bath, all washes occur on the benchtop at room temperature.]
2. Remove the SSCT, gently add 100 µl of RNAscope V2 Amp 1 solution (ACD) and incubate for 30 min at 40°C. [Note: All solutions should be added gently to reduce unnecessary disturbance to the fibers. We recommend tilting each tube to the side and slowly adding the solution down the side.]
3. Wash 3× with SSCT, then add 100 µl of RNAscope V2 Amp 2 solution (ACD) and incubate for 30 min at 40°C.
4. Wash 3× with SSCT, then add 150 µl of RNAscope V2 Amp 3 solution (ACD) and incubate for 15 min at 40°C.
5. Wash 3× with SSCT, then proceed with each individual channel. [Note: Using the RNAscope V2 kit is necessary for reducing background and overall signal-to-noise ratio but requires separate amplifications of each individual channel. Each probe is specific to a channel (C1, C2 or C3), and the amplification reagents used are specific to those channels.]
6. Gently add 150 µl of RNAscope HRP-C1 (or C2 or C3; this is dependent on which probes are being used) solution (ACD) and incubate for 15 min at 40°C.
7. Wash 3× with SSCT, then add 150 µl of diluted TSA+ fluorophore (PerkinElmer, 1:1000 in ACD-provided TSA buffer) and incubate for 30 min. [Note: You can mix and match channels and fluorophores, as well as changing the order of channel amplification. Although we have not observed a noticeable change in signal based on amplification order, you may need to increase the concentration of Cy5 fluorophore if performing additional channel amplification steps afterwards. This can be avoided by assigning the Cy5 fluorophore last.]
8. Wash 3× with SSCT, then add 150 µl of HRP-blocker solution and incubate for 15 min at 40°C. [Note: After fluorophores have been added to the fibers, the remaining steps must be carried out while keeping the fibers in the dark. How this is executed may vary, but we cover our tubes on the nutator with an opaque box and then allow them to stand upright in a closed drawer. Removal of solutions still requires backlighting to visualize the fibers, but if these steps are performed quickly the photobleaching is minimized.]
9. Wash 3× with SSCT, then repeat amplification (steps 6-8) for remaining channels if necessary.
10. After final SSCT washes, add 4-6 drops of RNAscope-provided DAPI solution to the tubes and incubate at 4°C overnight with slow agitation or mount immediately using Fluoromount with DAPI.

**MF-RNAscope/IF multiplexing (day 2 and day 3)****Protocol**

1. Perform RNAscope as described, following through the final HRP blocking. All of the following steps should be in the dark to minimize photobleaching; we use aluminum foil to block out light.
2. After final SSCT washes, wash fibers once with PBS for 6 min (3 min on nutator, 3 min standing).
3. Wash 3× with PBTX for 6 min.
4. Perform IF while maintaining fibers in Eppendorf tubes (protocol as previously described), beginning with the blocking step.

**Imaging and post-imaging analysis**

All microscopy was performed at the Microscopy CoRE at the Icahn School of Medicine at Mount Sinai. Images were acquired using Leica SP5 DM upright and Leica SP5 inverted confocal microscopes, both equipped with Leica Application Suite software and z-stacks were taken throughout the

depth of each fiber with a step size of 1 µm. Line averaging was used on all images to improve signal-to-noise ratio (line average=3, frame average=2). Images were exported to ImageJ and Fiji for quantifications, adjustment of brightness/contrast and generation of merged images.

**Image quantification****Transcript quantification in SCs**

For quantification of transcripts per SC, z-stacks were taken throughout the depth of SCs, with ≥25 SCs per mouse and ≥3 mice per target gene (exact *n*-values are stated in the figure legends). Transcripts were counted manually using Fiji's Cell Counter program on maximum intensity projections.

**Transcript quantification in myofibers**

For quantification of transcript counts/localizations within myofibers, three z-stacks (taken at 40× magnification, spanning the entire depth of the fiber) were analyzed per fiber, with 10 fibers analyzed per mouse and ≥3 mice (exact *n* values are stated in the figure legends). Images were processed in ImageJ software using the Threshold function, followed by quantification using Fiji's Analyze Particles program on maximum intensity projections (pixel size set from 0-∞, circularity from 0 to 1.0 to include all puncta). Nuclear transcripts and number of nuclei were counted manually using Fiji's Cell Counter program while moving through z-stacks; cytoplasmic transcripts were calculated by subtracting nuclear counts from the total numbers.

**Colocalization of Dll4 and GM130 fiber puncta**

A pipeline on CellProfiler (PMID: 17076895; Carpenter et al., 2006) was written that identified primary objects for both Dll4 and GM130 labeling, measured object overlap and used CellProfiler's precision parameter to quantify a ratio of: (number of Dll4 puncta that overlap with GM130 puncta)/(total number of Dll4 puncta). We quantified 52 images from *n*=3 mice.

**Quantification of Myod1 transcripts within myofibers**

Because the number of nuclei per fiber in each 40× image was not significantly different between T0 and T24 timepoints, a ratio of (number of RNA molecules within fibers)/(number of nuclei within a 40× fiber image) was used to standardize and calculate the level of transcripts within fibers. The average T0 calculation was plotted as 1, and the T24 calculation was determined accordingly.

**Acknowledgements**

We thank Susan Eliazar and Andrew Brack for sharing information on Dll4 before publication, Esperanza Agullo Pascual for her help with both image acquisition and quantification, and Paul Wasserman, Margaret Hung, and Denise Jurczyszak for critical reading of the manuscript.

**Competing interests**

The authors declare no competing or financial interests.

**Author contributions**

Conceptualization: A.P.K., R.S.K.; Methodology: A.P.K.; Formal analysis: A.P.K.; Investigation: A.P.K.; Writing - original draft: A.P.K.; Writing - review & editing: A.P.K., R.S.K.; Visualization: A.P.K.; Supervision: R.S.K.; Project administration: R.S.K.; Funding acquisition: A.P.K., R.S.K.

**Funding**

This work was funded by the National Institutes of Health [AR070231 to R.S.K.], a fellowship of the Training Program in Stem Cell Research from the New York State Department of Health [NYSTEM-C32561GG to A.P.K.], and the Tisch Cancer Institute at Icahn School of Medicine at Mount Sinai [P30 CA196521 – Cancer Center Support Grant]. Deposited in PMC for release after 12 months.

**Supplementary information**

Supplementary information available online at <http://dev.biologists.org/lookup/doi/10.1242/dev.179259.supplemental>

**References**

Beauchamp, J. R., Heslop, L., Yu, D. S. W., Tajbakhsh, S., Kelly, R. G., Wernig, A., Buckingham, M. E., Partridge, T. A. and Zammit, P. S. (2000). Expression of CD34 and Myf5 defines the majority of quiescent adult skeletal muscle satellite cells. *J. Cell Biol.* **151**, 1221-1234. doi:10.1083/jcb.151.6.1221

- Bischoff, R. (1986). Proliferation of muscle satellite cells on intact myofibers in culture. *Dev. Biol.* **115**, 129–139. doi:10.1016/0012-1606(86)90234-4
- Bjornson, C. R. R., Cheung, T. H., Liu, L., Tripathi, P. V., Steeper, K. M. and Rando, T. A. (2012). Notch signaling is necessary to maintain quiescence in adult muscle stem cells. *Stem Cells* **30**, 232–242. doi:10.1002/stem.773
- Brack, A. S. and Rando, T. A. (2012). Tissue-specific stem cells: Lessons from the skeletal muscle satellite cell. *Cell Stem Cell* **10**, 504–514. doi:10.1016/j.stem.2012.04.001
- Bruusgaard, J. C., Liestøl, K. and Gundersen, K. (2006). Distribution of myonuclei and microtubules in live muscle fibers of young, middle-aged, and old mice. *J. Appl. Physiol.* **100**, 2024–2030. doi:10.1152/jappphysiol.00913.2005
- Carpenter, A. E., Jones, T. R., Lamprecht, M. R., Clarke, C., Kang, I. H., Friman, O., Guertin, D. A., Chang, J. H., Lindquist, R. A., Moffat, J., Golland, P. and Sabatini, D. M. (2006). CellProfiler: image analysis software for identifying and quantifying cell phenotypes. *Genome Biol.* **7**, R100. doi:10.1186/gb-2006-7-10-r100
- Chakkalakal, J. V. and Jasin, B. J. (2002). Localizing synaptic mRNAs at the neuromuscular junction: it takes more than transcription. *BioEssays* **25**, 25–31. doi:10.1002/bies.10205
- Chakkalakal, J. V., Jones, K. M., Basson, M. A. and Brack, A. S. (2012). The aged niche disrupts muscle stem cell quiescence. *Nature* **490**, 355–360. doi:10.1038/nature11438
- Christov, C., Chrétien, F., Abou-Khalil, R., Bassez, G., Vallet, G., Authier, F.-J., Bassaglia, Y., Shinin, V., Tajbakhsh, S., Chazaud, B. et al. (2007). Muscle satellite cells and endothelial cells: close neighbors and privileged partners. *Mol. Biol. Cell* **18**, 1397–1409. doi:10.1091/mbc.e06-08-0693
- Collins, C. A., Zammit, P. S., Ruiz, A. P., Morgan, J. E. and Partridge, T. A. (2007). A population of myogenic stem cells that survives skeletal muscle aging. *Stem Cells* **25**, 885–894. doi:10.1634/stemcells.2006-0372
- Crist, C. G., Montarras, D. and Buckingham, M. (2012). Muscle satellite cells are primed for myogenesis but maintain quiescence with sequestration of Myf5 mRNA targeted by microRNA-31 in mRNP granules. *Cell Stem Cell* **11**, 118–126. doi:10.1016/j.stem.2012.03.011
- De Morée, A., van Velthoven, C. T. J., Gan, Q., Salvi, J. S., Klein, J. D. D., Akimenko, I., Quarta, M., Biressi, S. and Rando, T. A. (2017). Staufen1 inhibits MyoD translation to actively maintain muscle stem cell quiescence. *Proc. Natl. Acad. Sci. USA* **114**, E8996–E9005. doi:10.1073/pnas.1708725114
- Dell'Orso, S., Juan, A. H., Ko, K.-D., Naz, F., Perovanovic, J., Gutierrez-Cruz, G., Feng, X. and Sartorelli, V. (2019). Single-cell analysis of adult skeletal muscle stem cells in homeostatic and regenerative conditions. *Development* **146**, dev174177. doi:10.1242/dev.174177
- Dumont, N. A., Wang, Y. X. and Rudnicki, M. A. (2015). Intrinsic and extrinsic mechanisms regulating satellite cell function. *Development* **142**, 1572–1581. doi:10.1242/dev.114223
- Fontaine, B., Sassoon, D., Buckingham, M. and Changeux, J. P. (1988). Detection of the nicotinic acetylcholine receptor  $\alpha$ -subunit mRNA by *in situ* hybridization at neuromuscular junctions of 15-day-old chick striated muscles. *EMBO J.* **7**, 603–609. doi:10.1002/j.1460-2075.1988.tb02853.x
- Fukada, S.-I., Yamaguchi, M., Kokubo, H., Ogawa, R., Uezumi, A., Yoneda, T., Matev, M. M., Motohashi, N., Ito, T., Zolkiewska, A. et al. (2011). Hes1 and Hes3 are essential to generate undifferentiated quiescent satellite cells and to maintain satellite cell numbers. *Development* **138**, 4609–4619. doi:10.1242/dev.067165
- Gayraud-Morel, B., Le Bouteiller, M., Commere, P.-H., Cohen-Tannoudji, M. and Tajbakhsh, S. (2018). Notchless defines a stage-specific requirement for ribosome biogenesis during lineage progression in adult skeletal myogenesis. *Development* **145**, dev162636. doi:10.1242/dev.162636
- Goel, A. J. and Krauss, R. S. (2018). Ex vivo visualization and analysis of the muscle stem cell niche. In *Stem Cell Niche (Methods in Molecular Biology)* (ed. K. Turksen), pp. 39–50. Humana. doi:10.1007/978-1-4939-9817-7\_1
- Goel, A. J., Rieder, M.-K., Arnold, H.-H., Radice, G. L. and Krauss, R. S. (2017). Niche cadherins control the quiescence-to-activation transition in muscle stem cells. *Cell Rep.* **21**, 2236–2250. doi:10.1016/j.celrep.2017.10.102
- Gross-Thebing, T., Paksa, A. and Raz, E. (2014). Simultaneous high-resolution detection of multiple transcripts combined with localization of proteins in whole-mount embryos. *BMC Biol.* **12**, 55. doi:10.1186/s12915-014-0055-7
- Hausburg, M. A., Doles, J. D., Clement, S. L., Cadwallader, A. B., Hall, M. N., Blackshear, P. J., Lykke-Andersen, J. and Olwin, B. B. (2015). Post-transcriptional regulation of satellite cell quiescence by TTP-mediated mRNA decay. *eLife* **4**, e03390. doi:10.7554/eLife.03390
- Irintchev, A., Zeschnigk, M., Starzinski-Powitz, A. and Wernig, A. (1994). Expression pattern of M-cadherin in normal, denervated, and regenerating mouse muscles. *Dev. Dyn.* **199**, 326–337. doi:10.1002/aja.1001990407
- Jasmin, B. J., Lee, R. K. and Rotundo, R. L. (1993). Compartmentalization of acetylcholinesterase mRNA and enzyme at the vertebrate neuromuscular junction. *Neuron* **11**, 467–477. doi:10.1016/0896-6273(93)90151-G
- Jevsek, M., Jaworski, A., Polo-Parada, L., Kim, N., Fan, J., Landmesser, L. T. and Burden, S. J. (2006). CD24 is expressed by myofiber synaptic nuclei and regulates synaptic transmission. *Proc. Natl. Acad. Sci. USA* **103**, 6374–6379. doi:10.1073/pnas.0601468103
- Keire, P., Shearer, A., Shefer, G. and Yablonka-Reuveni, Z. (2013). Isolation and culture of skeletal muscle myofibers as a means to analyze satellite cells. In *Basic Cell Culture Protocols, Methods in Molecular Biology*, Vol. 946 (eds C. D. Helgason and C. L. Miller), pp. 431–466. New York, NY: Springer.
- Kersigo, J., Pan, N., Lederman, J. D., Chatterjee, S., Abel, T., Pavlinkova, G., Silos-Santiago, I. and Fritzsche, B. (2018). A RNAscope whole mount approach that can be combined with immunofluorescence to quantify differential distribution of mRNA. *Cell Tissue Res.* **374**, 251–262. doi:10.1007/s00441-018-2864-4
- Krauss, R. S., Joseph, G. A. and Goel, A. J. (2017). Keep your friends close: cell-cell contact and skeletal myogenesis. *Cold Spring Harb. Perspect. Biol.* **9**, a029298. doi:10.1101/cshperspect.a029298
- Kuang, S., Kuroda, K., Le Grand, F. and Rudnicki, M. A. (2007). Asymmetric self-renewal and commitment of satellite stem cells in muscle. *Cell* **129**, 999–1010. doi:10.1016/j.cell.2007.03.044
- Kuang, S., Gillespie, M. A. and Rudnicki, M. A. (2008). Niche regulation of muscle satellite cell self-renewal and differentiation. *Cell Stem Cell* **2**, 22–31. doi:10.1016/j.stem.2007.12.012
- Machado, L., Esteves, de Lima, J., Fabre, O., Proux, C., Legendre, R., Szegedi, A., Varet, H., Ingerslev, L. R., Barrès, R. et al. (2017). *In situ* fixation redefines quiescence and early activation of skeletal muscle stem cells. *Cell Rep.* **21**, 1982–1993. doi:10.1016/j.celrep.2017.10.080
- Mashinchian, O., Pisconti, A., Le Moal, E. and Bentzinger, C. F. (2018). Chapter two – The muscle stem cell niche in health and disease. *Curr. Top. Dev. Biol.* **126**, 23–65. doi:10.1016/bs.ctdb.2017.08.003
- Merlie, J. P. and Sanes, J. R. (1985). Concentration of acetylcholine receptor mRNA in synaptic regions of adult muscle fibres. *Nature* **317**, 66–68. doi:10.1038/317066a0
- Mitsui, T., Kawai, H., Shono, M., Kawajiri, M., Kunishige, M. and Saito, S. (1997). Preferential subsarcolemmal localization of dystrophin and  $\beta$ -dystroglycan mRNA in human skeletal muscles. *J. Neuropathol. Exp. Neurol.* **56**, 94–101. doi:10.1097/00005072-199701000-00010
- Moscato, L. M., Merlie, J. P. and Sanes, J. R. (1995). N-CAM, 43K-rapsyn, and S-laminin mRNAs are concentrated at synaptic sites in muscle fibers. *Mol. Cell Neurosci.* **6**, 80–89. doi:10.1006/mcne.1995.1008
- Mourikis, P., Sambasivan, R., Castel, D., Rocheteau, P., Bizzarro, V. and Tajbakhsh, S. (2012). A critical requirement for notch signaling in maintenance of the quiescent skeletal muscle stem cell state. *Stem Cells* **30**, 243–252. doi:10.1002/stem.775
- Nevalainen, M., Kaisto, T. and Metsikkö, K. (2010). Mobile ER-to-Golgi but not post-Golgi membrane transport carriers disappear during the terminal myogenic differentiation. *Cell Tissue Res.* **342**, 107–116. doi:10.1007/s00441-010-1041-1
- Nissinen, M., Kaisto, T., Salmela, P., Peltonen, J. and Metsikkö, K. (2005). Reduced distribution of mRNAs encoding a sarcoplasmic reticulum or transverse tubule protein in skeletal myofibers. *J. Histochem. Cytochem.* **53**, 217–227. doi:10.1369/jhc.4A6431.2005
- Olguin, H. C. and Olwin, B. B. (2004). Pax-7 up-regulation inhibits myogenesis and cell cycle progression in satellite cells: a potential mechanism for self-renewal. *Dev. Biol.* **275**, 375–388. doi:10.1016/j.ydbio.2004.08.015
- Pallafacchina, G., François, S., Regnault, B., Czarny, B., Dive, V., Cumano, A., Montarras, D. and Buckingham, M. (2010). An adult tissue-specific stem cell in its niche: A gene profiling analysis of *in vivo* quiescent and activated muscle satellite cells. *Stem Cell Res.* **4**, 77–91. doi:10.1016/j.scr.2009.10.003
- Rocheteau, P., Gayraud-Morel, B., Siegl-Cachedenier, I., Blasco, M. A. and Tajbakhsh, S. (2012). A subpopulation of adult skeletal muscle stem cells retains all template DNA strands after cell division. *Cell* **148**, 112–125. doi:10.1016/j.cell.2011.11.049
- Rosenblatt, J. D., Lunt, A. I., Parry, D. J. and Partridge, T. A. (1995). Culturing satellite cells from living single muscle fiber explants. *In Vitro Cell. Dev. Biol. Anim.* **31**, 773–779. doi:10.1007/BF02634119
- Rossi, S. G. and Rotundo, R. L. (1992). Cell surface acetylcholinesterase molecules on multinucleated myotubes are clustered over the nucleus of origin. *J. Cell Biol.* **119**, 1657–1667. doi:10.1083/jcb.119.6.1657
- Rotundo, R. L. (1990). Nucleus-specific translation and assembly of acetylcholinesterase in multinucleated muscle cells. *J. Cell Biol.* **110**, 715–719. doi:10.1083/jcb.110.3.715
- Sampath, S. C., Sampath, S. C., Ho, A. T. V., Corbel, S. Y., Millstone, J. D., Lamb, J., Walker, J., Kinzel, B., Schmedt, C. and Blau, H. M. (2018). Induction of muscle stem cell quiescence by the secreted niche factor Oncostatin M. *Nat. Commun.* **9**, 1531. doi:10.1038/s41467-018-03876-8
- Sanes, J. R., Johnson, Y. R., Kotzbauer, P. T., Mudd, J., Hanley, T., Martinou, J. C. and Merlie, J. P. (1991). Selective expression of an acetylcholine receptor-lacZ transgene in synaptic nuclei of adult muscle fibers. *Development* **113**, 1181–1191.
- Shinin, V., Gayraud-Morel, B., Gomès, D. and Tajbakhsh, S. (2006). Asymmetric division and cosegregation of template DNA strands in adult muscle satellite cells. *Nat. Cell Biol.* **8**, 677–682. doi:10.1038/ncb1425
- Shoemaker, S. D., Ryan, A. F. and Lieber, R. L. (1999). Transcript-specific mRNA trafficking based on the distribution of coexpressed myosin isoforms. *Cell Tissues Organs* **165**, 10–15. doi:10.1159/000016668



- Tanaka, K. K., Hall, J. K., Troy, A. A., Cornelison, D. D. W., Majka, S. M. and Olwin, B. B.** (2009). Syndecan-4-expressing muscle progenitor cells in the SP engraft as satellite cells during muscle regeneration. *Cell Stem Cell* **4**, 217-225. doi:10.1016/j.stem.2009.01.016
- Tassin, A.-M., Maro, B. and Bornens, M.** (1985). Fate of microtubule-organizing centers during myogenesis in vitro. *J. Cell Biol.* **100**, 35-46. doi:10.1083/jcb.100.1.35
- van Velthoven, C. T. J., de Morrée, A., Egner, I. M., Brett, J. O. and Rando, T. A.** (2017). Transcriptional profiling of quiescent muscle stem cells *in vivo*. *Cell Rep.* **21**, 1994-2004. doi:10.1016/j.celrep.2017.10.037
- Vogler, T., Gadek, K. E., Cadwallader, A. B., Elston, T. L. and Olwin, B. B.** (2016). Isolation, culture, functional assays, and immunofluorescence of myofiber-associated satellite cells. In *Skeletal Muscle Regeneration in the Mouse: Methods and Protocols, Methods in Molecular Biology*, Vol. 1460 (ed. M. Kyba), pp.141-162. New York, NY: Springer.
- Wang, F., Flanagan, J., Su, N., Wang, L.-C., Bui, S., Nielson, A., Wu, X., Vo, H.-T., Ma, X.-J. and Luo, Y.** (2012). RNAscope: a novel in situ RNA analysis platform for formalin-fixed, paraffin-embedded tissues. *J. Mol. Diagn.* **14**, 22-29. doi:10.1016/j.jmoldx.2011.08.002
- Zammit, P. S., Golding, J. P., Nagata, Y., Hudon, V., Partridge, T. A. and Beauchamp, J. R.** (2004). Muscle satellite cells adopt divergent fates: a mechanism for self-renewal? *J. Cell Biol.* **166**, 347-357. doi:10.1083/jcb.200312007

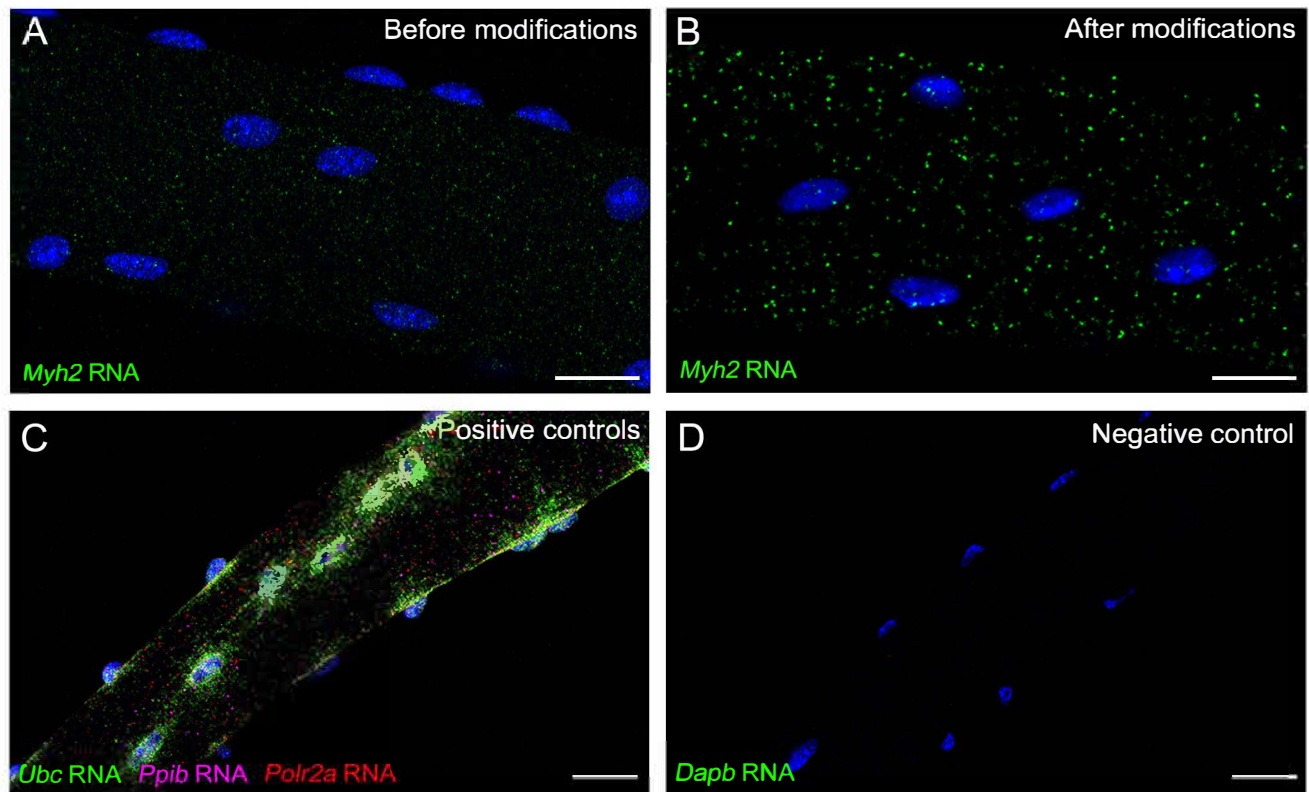


**Figure S1. MF-RNAscope allows sensitive detection of single transcripts in whole-mount muscle fibers.**

(A,B) MF-RNAscope of freshly isolated EDL fibers probed for *Myh2* RNA, shown (A) before and (B) after modifications to the manufacturer's V2 system protocol, as presented in the paper.

(C,D) MF-RNAscope of isolated EDL fibers probed for (C) manufacturer-provided positive control genes *Ubc*, *Ppib*, and *Polr2a* and (D) negative control bacterial gene *Dapb*.

Scale bars: (A,B) 20 $\mu$ m; (C,D) 25 $\mu$ m. Nuclei are identified with DAPI.

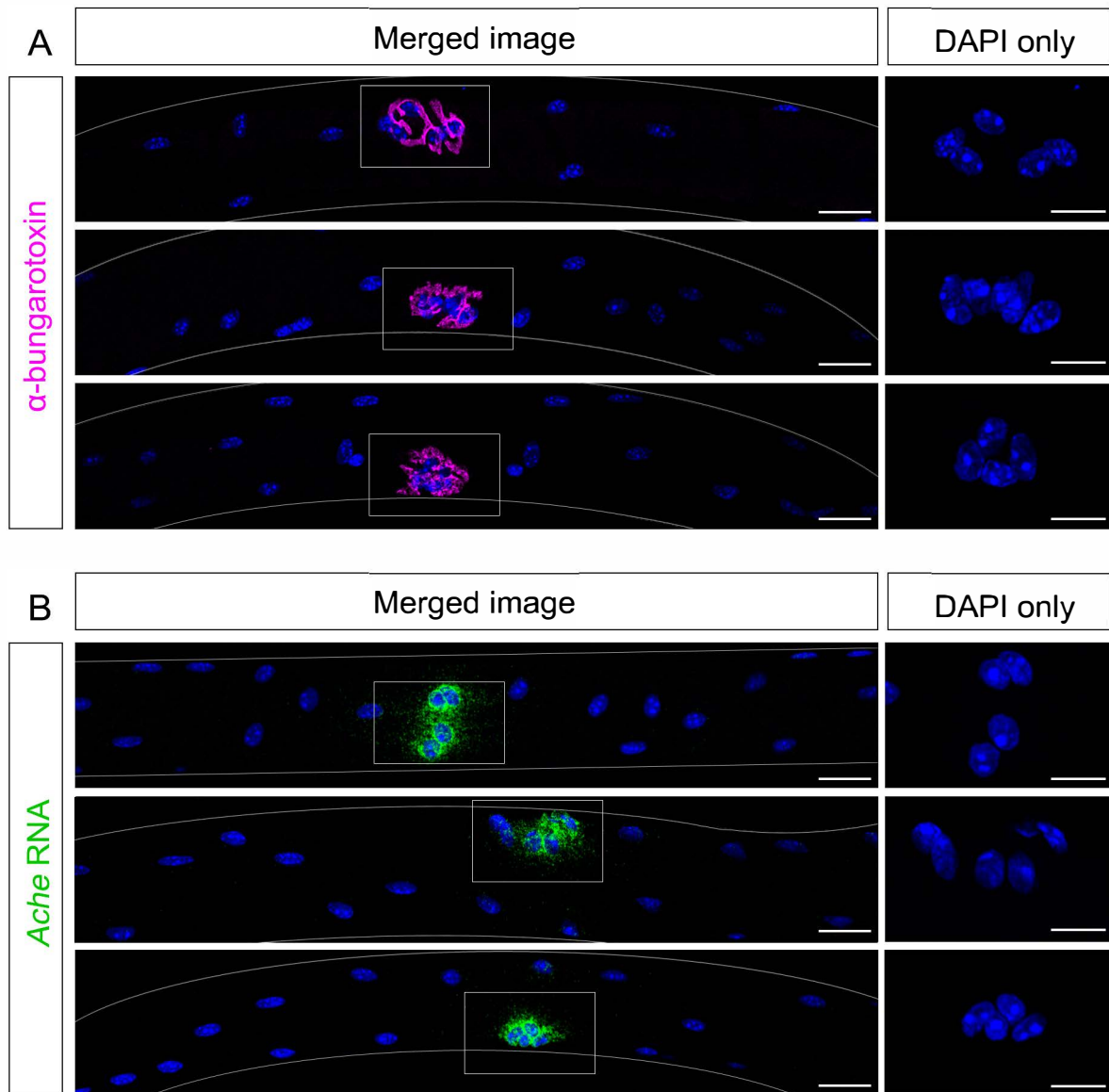


**Figure S2. *Ache* transcripts are specifically localized around the NMJ.**

(A,B) Synaptic myonuclei organize in distinctive clusters on myofibers and can be labeled by (A)  $\alpha$ -bungarotoxin (magenta) or (B) *Ache* RNA (green). Insets on the right show DAPI-stained clusters of synaptic myonuclei. We note that these clusters of myonuclei are unique to the postsynaptic side of the NMJ (therefore only one per myofiber is observed), and DAPI staining alone is sufficient for their identification.

Scale bars: (A,B) 25 $\mu$ m (A,B insets) 20 $\mu$ m.



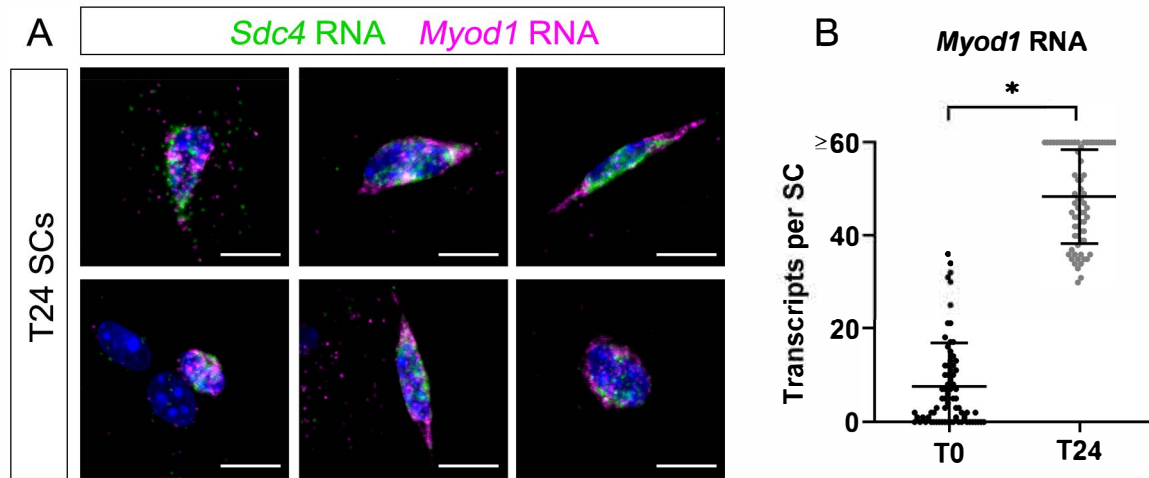


**Figure S3. *Myod1* transcripts in SCs are upregulated upon activation.**

(A) MF-RNAscope of EDL fibers cultured with CEE for 24 hours, probed for *Sdc4* (green) and *Myod1* (magenta) RNAs. Images are maximum intensity projections of confocal images throughout each SC. (B) Quantification of *Myod1* transcripts at T0 (data from Figure 2B) and T24. Mean  $\pm$  SD.  $n=73$  (T0) or  $n=70$  (T24) SCs from 3 mice each. \* =  $p<0.0001$  using a two-tailed unpaired  $t$ -test.

Scale bars: (all) 10  $\mu$ m. All nuclei are identified with DAPI.

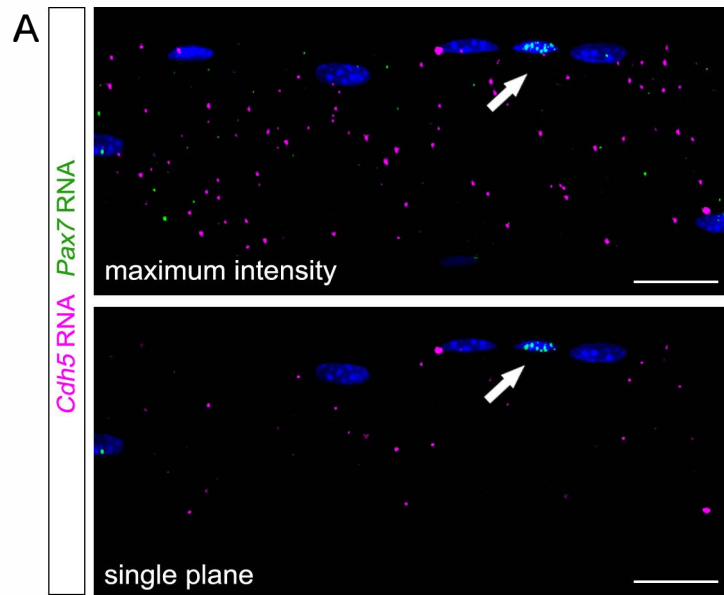


**Figure S4. *Cdh5* transcripts are distributed evenly throughout the length and depth of myofibers.**

(A) MF-RNAscope of single EDL fibers probed for *Pax7* (green) and *Cdh5* (magenta) RNAs. Top image shows a maximum intensity projection of confocal images throughout a myofiber section (40x magnification); z-stack distance = 0.5μm. Bottom image shows a single confocal plane. Arrows indicate a Pax7<sup>+</sup> SC.

Scale bars: (all) 25μm. Nuclei are identified with DAPI.

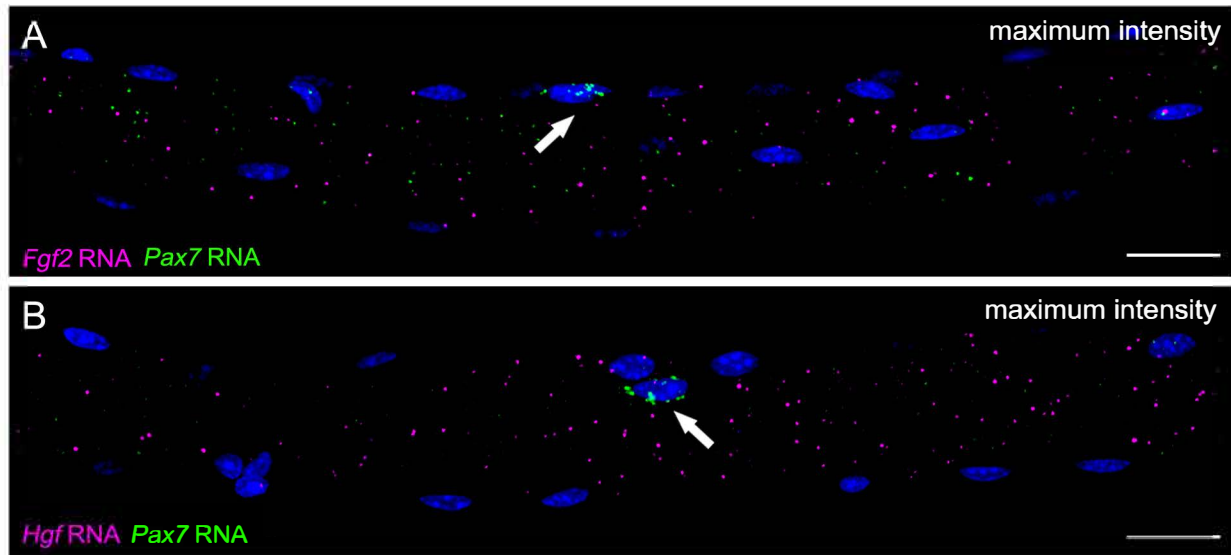


**Figure S5. *Fgf2* and *Hgf* transcripts are distributed throughout myofibers.**

(A,B) MF-RNAscope of single EDL fibers probed for *Pax7* (green) and either (A) *Fgf2* or (B) *Hgf* (magenta). Images are maximum intensity projections of confocal images throughout each myofiber section (40x magnification); z-stack distance = 1 μm. Arrows indicate *Pax7*<sup>+</sup> SCs. Scale bars: (all) 25 μm. Nuclei are identified with DAPI.



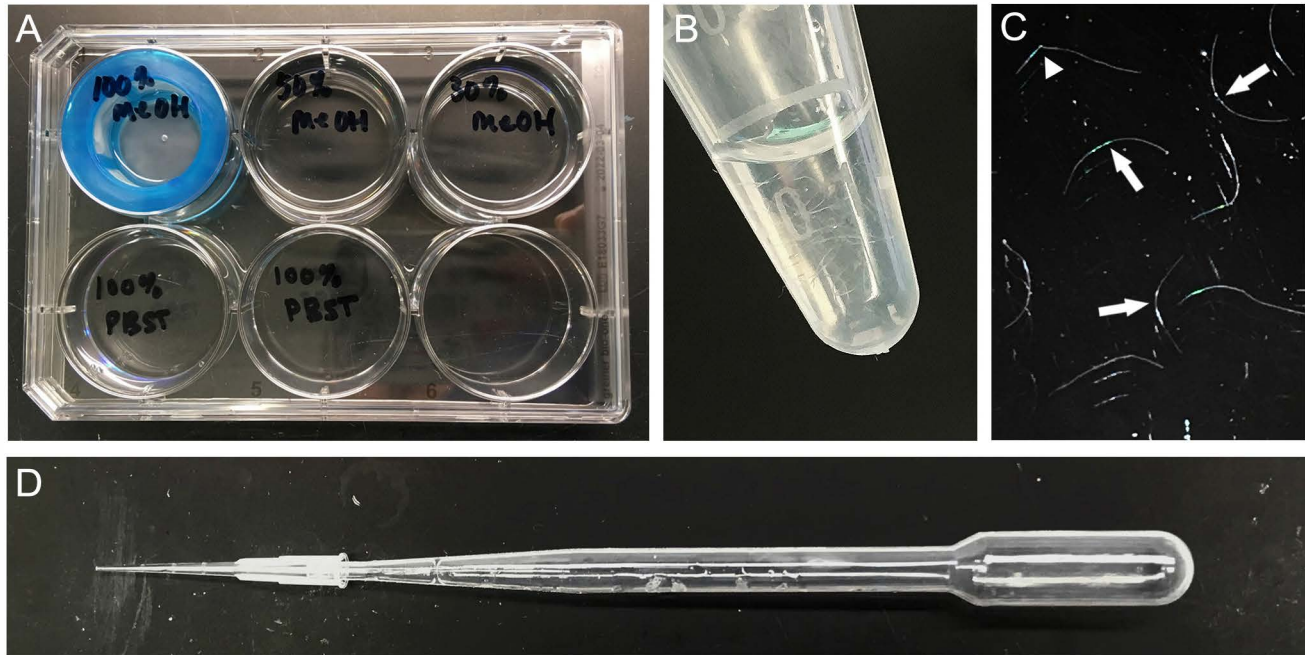


**Figure S6. Tools used during the MF-RNAscope protocol.**

(A) Rehydration set-up showing a 40µm nylon filter in a 6-well untreated tissue culture plate containing 100% MeOH, 50% MeOH/50% PBST, 30% MeOH/70% PBST, and 100% PBST. (B) Visibility of myofibers in Axygen 1.7mL tubes. (C) Examples of rehydrated myofibers. Arrows indicate healthy intact myofibers, arrowhead indicates a kinked myofiber; the former perform well with MF-RNAscope, the latter do not. (D) Transfer apparatus comprised of a 10µl pipette tip on the end of a transfer pipette.

**Table S1: Reagents used****Antibodies:**

Antibody	Host	Isotype	Concentration	Manufacturer	Product #
Pax7	Mouse	IgG1	1:100	DSHB	PAX7c
Caveolin-1	Rabbit	IgG	1:750	Abcam	ab2910
M-cadherin	Mouse	IgG1	1:50	Santa Cruz	12G4
Dll-4	Rabbit	IgG	1:500	Abcam	ab7280
GM130	Mouse	IgG1k	1:50	BD Biosciences	610822
$\alpha$ -Bungarotoxin, Alexa594-conjugated			1:100	ThermoFisher	B13423
goat Alexa488-conjugated anti-mouse IgG1			1:300	Thermofisher	A-21121
goat Alexa568-conjugated anti-rabbit IgG			1:300	Thermofisher	A-11011
goat Alexa647-conjugated anti-mouse IgG1			1:300	Invitrogen	A21240

**Benchtop reagents:**

Reagent	Composition
4% PFA	Filtered 1X PBS + Electron Microscopy Sciences Paraformaldehyde
PBTX	RNase-free 1X PBS + 0.2% Triton-X-100 (filter before use)
PBST	RNase-free 1X PBS + 0.01% Tween-20 (filter before use)
SSCT	RNase-free 0.2X saline-sodium citrate buffer + 0.01% Tween-20 (filter before use)

**RNAscope reagents:**

Reagent	Reference #
RNAscope Multiplex Fluorescent Detection Reagents v2	323110
RNAscope Protease III	322381
RNAscope Probe – Mm-Cdh2 (C1)	489571
RNAscope Probe – Mm-Cdh5 (C1)	312531
RNAscope Probe – Mm-Dll4 (C1)	319971
RNAscope Probe – Mm-Myod1 (C1)	316081
RNAscope Probe – Mm-Myh2 (C1)	401401
RNAscope Probe – Mm-Myf5 (C1)	492911
RNAscope Probe – Mm-Fgf2 (C1)	316851
RNAscope Probe – Mm-Hgf (C1)	315631
RNAscope Probe – Mm-Sdc4 (C1)	473591
RNAscope Probe – Mm-Cdh15 (C2)	473711-C2
RNAscope Probe – Mm-Ache (C2)	490021-C2
RNAscope Probe – Mm-Myod1 (C2)	316081-C2
RNAscope Probe – Mm-Vcam1 (C2)	438641-C2
RNAscope Probe – Mm-Cd34 (C2)	319161-C2
RNAscope Probe – Mm-Pax7 (C3)	314181-C3
RNAscope Probe Diluent	300041
RNAscope TSA Buffer	322809
PerkinElmer TSA Plus Fluorescein System	NEL741001
PerkinElmer TSA Plus Cyanine 5 System	NEL745001



**Movie 1. MF-RNAscope permeates throughout the entire depth of myofibers.**

Detection of *Ache* (green) and *Myh2* (magenta) RNAs throughout a myofiber using MF-RNAscope. Video is a confocal z-stack of the NMJ taken at 120x magnification; z-step distance between images = 0.5 $\mu$ m.